Supplementary Information

Speciation and Partitioning: A Survey Study of Rare Earth Elements (REEs) in Coal Fly Ash

Estefania Garcia, Yinghao Wen, Pan Liu, Yuanzhi Tang*

School of Earth and Atmospheric Sciences, Georgia Institute of Technology, 311 Ferst Drive, Atlanta, Georgia 30332, USA

* Corresponding author:

Yuanzhi Tang: yuanzhi.tang@eas.gatech.edu

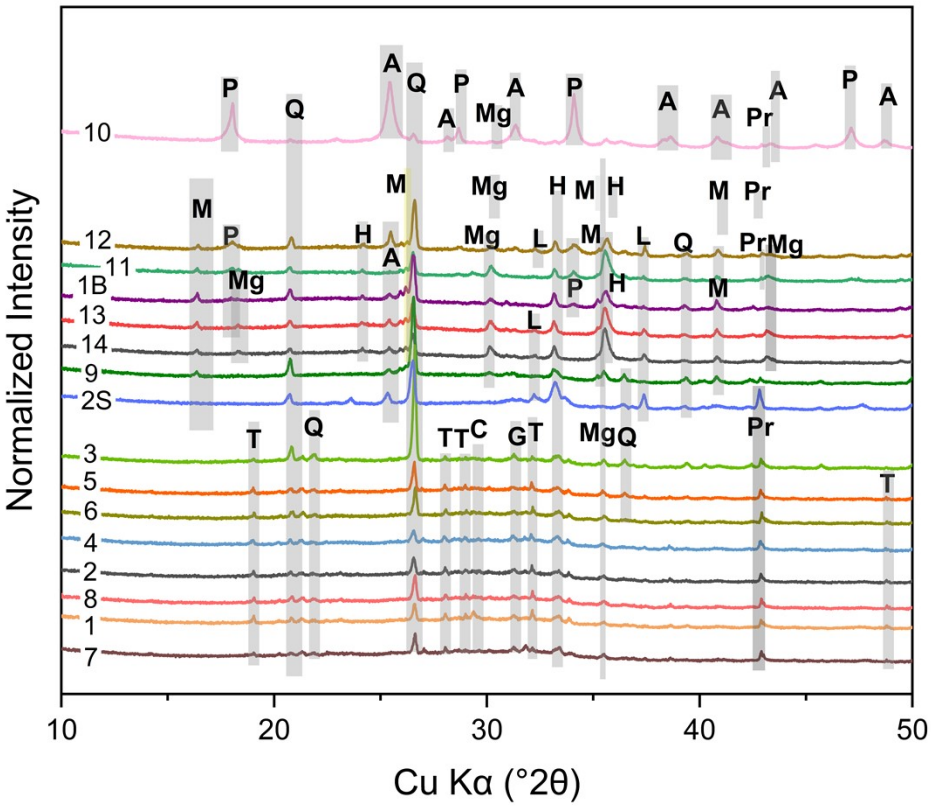

Figure S1. XRD spectra with corresponding sample labels on the left and peak assignments in gray bars. Mullite (M), Portlandite (P), Magnetite (Mg), Thenardite (T), Quartz (Q), Hematite (H), Anhydrite (A), Calcite (C), Gehlenite (G), Lime (L), and Periclase (Pr).[1, 2]

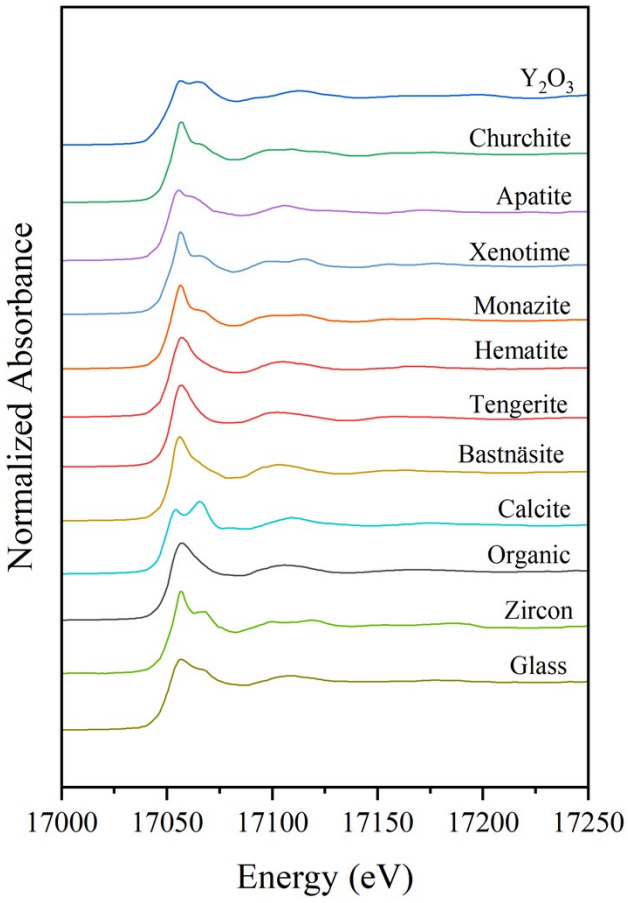

Figure S2. Y K-edge XANES spectra of model compounds.

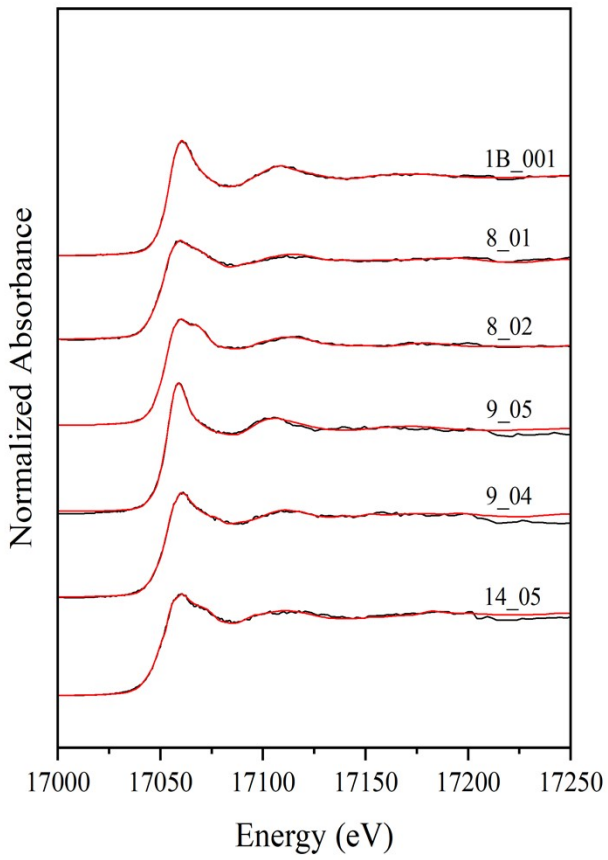

Figure S3. Y K-edge μ-XANES spectra (black) of selected CFAs and their corresponding LCF fits (red). μ-XANES spectra for samples 1B, 8, 9, and 14.

Table S1. Bulk composition properties of CFA samples.[1]

Sample ID	Major element (wt%)				Average particle size (μm)	Surface Area (cm^2/cm^3)	Bulk density (mg/cc)	LOI
	Fe_2O_3	Al_2O_3	SiO_2	CaO				
1	5.27	20.49	38.95	19.72	13.2	9724.7	2.63	1.75
2	5.26	20.06	40.92	18.65	12.7	8917.9	2.56	0.91
3	6.73	16.88	49.12	15.6	51.4	4271.7	2.53	0.86
4	5.44	19.99	40.2	19.19	11.5	9735.4	2.59	1.05
5	5.69	20.95	41.18	17.56	14.0	9972.8	2.59	0.76
6	5.66	21.07	40.82	17.73	13.5	9780.5	2.57	0.71
7	5.28	20.46	38.91	19.79	10.1	10022	2.61	0.95
8	5.68	20.9	41.17	17.52	13.7	9867.3	2.56	0.66
9	9.84	21.84	44.45	17.07	21.2	9233.7	2.56	3.41
10	9.95	11.24	24.13	51.61	8.3	16478	2.53	9.72
11	30.26	17.42	42.12	8.49	107.5	892.15	2.41	1.66
12	15.87	19.15	46.36	13.31	17.4	7314.3	2.48	2.43
13	24.13	22.89	42.9	7.47	41.3	3623.2	2.56	8.86
14	28.36	21.48	40.92	7.49	42.6	3514.8	2.69	3.96
1B	17.48	22.56	51.04	4.94	30.2	4996.1	2.37	0.42
2S	6.22	17.14	37.78	28.68	23.9	7017.8	2.69	3.07

Table S2. REE concentrations in CFA samples.

Sample ID	REE concentration (ppm)																Total REE
	Sc ± 1.7	Y ± 0.7	Tb ± 1.8	Dy ± 1.2	Ho ± 1.1	Er ± 1.2	Tm ± 1.7	Yb ± 1.1	Lu ± 1.9	La ± 0.6	Ce ± 0.6	Pr ± 0.8	Nd ± 1.0	Sm ± 1.5	Eu ± 1.3	Gd ± 1.1	
1	21.9	43.9	1.2	7.1	1.5	4.0	0.6	3.8	0.6	0.6	83.4	10.1	39.1	7.9	1.7	7.6	278.2
2	21.6	43.4	1.2	7.0	1.5	4.0	0.6	3.8	0.6	0.6	82.7	10.0	38.6	7.8	1.7	7.5	275.5
3	18.2	38.2	1.1	6.2	1.3	3.6	0.5	3.5	0.6	0.6	72.5	8.8	33.6	6.8	1.5	6.6	240.6
4	21.7	43.6	1.2	7.1	1.5	4.0	0.6	3.9	0.6	0.6	83.0	10.0	38.7	7.9	1.7	7.6	276.7
5	24.6	48.8	1.4	8.1	1.7	4.5	0.7	4.3	0.7	0.7	91.9	11.1	42.7	8.8	1.9	8.5	307.8
6	25.0	49.1	1.4	8.1	1.7	4.6	0.7	4.4	0.7	0.7	92.1	11.1	43.0	8.9	1.9	8.6	309.6
7	22.0	43.6	1.2	7.1	1.5	4.1	0.6	3.9	0.6	0.6	85.2	10.3	39.2	8.0	1.7	7.7	281.7
8	24.6	48.6	1.4	8.0	1.7	4.6	0.7	4.3	0.7	0.7	91.7	11.0	42.5	8.6	1.9	8.5	306.8
9	26.0	62.4	1.8	10.5	2.1	5.8	0.9	5.4	0.8	0.8	131.2	16.0	62.2	12.6	2.7	12.1	419.7
10	11.8	27.3	0.8	4.3	0.9	2.5	0.4	2.3	0.3	0.3	44.1	5.3	20.8	4.6	1.0	4.61	152.0
11	21.7	49.2	1.4	8.2	1.7	4.6	0.7	4.4	0.7	0.7	101.4	12.1	47.2	9.6	2.0	9.0	322.3
12	22.6	49.4	1.4	8.2	1.7	4.8	0.7	4.6	0.7	0.7	104.3	12.2	46.4	9.2	1.9	8.6	329.2
13	22.6	44.1	1.4	7.9	1.6	4.3	0.6	3.9	0.6	0.6	111.0	13.1	50.0	10.2	2.1	9.4	337.4
14	22.1	44.1	1.4	7.8	1.6	4.2	0.6	3.9	0.6	0.6	110.7	12.9	49.3	9.9	2.1	9.2	334.3
1B	30.7	64.4	1.9	10.8	2.2	2.2	6.1	0.9	5.6	62.0	127.5	15.0	57.9	12.0	2.6	11.8	403.2
2S	20.3	60.7	1.8	10.4	2.1	5.7	0.9	5.3	0.8	64.8	126.2	15.7	61.4	12.6	2.8	12.0	412.2

Table S3. Summary of Y model compounds for XANES analysis (from Liu et al.[3])

Reference compound	**Source or preparation method**
Y_2O_3	Sigma Aldrich
Churchite	$YPO_4 \cdot H_2O$ was synthesized by co-precipitation of Y^{3+} and PO_4^{3-} with molar ratio of 1:1[4]
Tengerite	$Y_2(CO_3)_3 \cdot 2\text{-}3H_2O$ from Sigma Aldrich
Apatite	$Ca_5(PO_4)_3(F,OH)$, natural mineral from Georgia, USA
Bastnäsite	$(Ce, La, Nd)CO_3(F, OH)$, natural mineral from Pakistan
Calcite	Y-doped calcite synthesized by Elzinga et al.[5]
Hematite	100 μM YCl_3 were added during hematite synthesis[6]
Glass	100 μM YCl_3 were added during glass synthesis[7]
Monazite	$(Ce, Th, La, Nd)PO_4$, natural mineral from New Mexico, USA
Xenotime	$(Y, Dy)PO_4$, natural mineral from California, USA
Zircon	$ZrSiO_4$, natural mineral from India
Organic	20 mL 100 μM $CeCl_3$, $NdCl_3$, and YCl_3 complexing with 0.5 g chitosan at pH 6.8 and freeze dried

Table S4. Linear combination fitting results (% contribution of individual phases) of Y K-edge μ-XANES data. The first number of the sample label corresponds to the CFA sample. Tengerite ($Y_2(CO_3)_3 \cdot 2–3H_2O$), Churchite ($YPO_4 \cdot H_2O$).

Sample	Y_2O_3	Tengerite	Glass	Calcite	Zircon	Churchite	Hematite	Organic	Monazite	Apatite	Xenotime	Sum	R-factor
2S_11	35.5 ± 4.5				62.0 ± 4.3							97.5	0.008975
2S_12	37.2 ± 3.5	17.6 ± 3.6			42.6 ± 5.4							97.4	0.005211
1B_01	25 ± 0.4						67.0 ± 1.1			2.5 ± 0.4	27.0 ± 1.1	99.0	0.0004127
1B_02	79.3 ± 4.3					17.9 ± 4.3						97.2	0.011374
1B_03			90.2 ± 5.9	4.2 ± 5.8								94.4	0.016531
1B_04	85.1 ± 4.5					11.4 ± 4.5						96.5	0.012712
1B_05	96.4 ± 3.7											96.4	0.010264
1B_06	84.2 ± 3.1	10.7 ± 3.0										94.9	0.010813
8_01	58.9 ± 9.8				28.8 ± 9.8		2.5 ± 9.8		9.0 ± 9.8			99.2	0.0009306
8_02	5.5 ± 0.4				37.0 ± 2.2					46.1 ± 1.5	11.5 ± 2.3	100.1	0.0004032
8_03	96.9 ± 9.1											96.9	0.027948
8_04			73.3 ± 12.2		22.0 ± 11.9							95.3	0.034354
8_05	94.2 ± 3.8											94.2	0.018243
8_06	93.3 ± 5.4											93.3	0.019553
9_01	81.7 ± 7.7					18.8 ± 7.6						100.5	0.032223
9_03	89.2 ± 10.2											89.2	0.065945
9_04	41.5 ± 1.4						47.2 ± 1.2		10.3 ± 0.3	4.2 ± 0.3		103.2	0.0008354
9_05	5.0 ± 0.7		0.1 ± 0.2				92.6 ± 3.6				8.0 ± 3.9	105.6	0.0012274
12_01	93.1 ± 4.2											93.1	0.022352
12_02	93.6 ± 5.5											93.6	0.018063
12_03			75.7 ± 8.4	15.2 ± 8.3								90.9	0.036760
14_01	93.9 ± 5.2											93.9	0.018892
14_02	81.6 ± 3.5		13.9 ± 3.4									95.5	0.014411
14_03	91.9 ± 9.1											91.9	0.035215
14_05	42.0 ± 1.4				4.4 ± 0.4		35.6 ± 1.1		20.9 ± 0.9			102.8	0.0012806
5_12	83.8 ± 4.0					11.6 ± 3.9						95.4	0.017683
5_14	77.5 ± 4.9				27.0± 4.6							104.5	0.016265
5_15	67.3 ± 4.4					25.2 ± 4.3						92.5	0.022288
10_11	54.7 ± 1.8					44.6 ± 2.5						99.3	0.006768
10_13	49.1 ± 4.1					49.0 ± 4.0						98.1	0.016466
10_14	49.8 ± 4.0					50.6 ± 3.8							0.014712
10_22	68.1 ± 4.1	35.0 ± 3.8										103.1	0.020226
11_14	57.8 ± 4.3	46.7 ± 4.0										104.5	0.021959
11_13	64.5 ± 3.7	32.8 ± 3.5										97.3	0.019337
11_15	60.4 ± 3.8	37.3± 3.6										97.7	0.019791
11_21	67.3 ± 3.8	21.7 ± 3.5										89.0	0.024639

11_22	66.1 ± 3.6	30.9 ± 3.4										97.0	0.01825
11_23	30.5 ± 4.0					68.7 ± 3.9						99.2	0.015047
11_24	49.7 ± 5.0						47.3 ± 4.6					96.0	0.021295
11_25	57.6 ± 6.2					48.8 ± 6.0						106.4	0.030543
13_11	70.0 ± 3.3	27.3 ± 3.3										97.3	0.015821
13_12	53.0 ± 4.2					54.0 ± 4.1						107.0	0.014495
13_13	41.8 ± 5.4							60.3 ± 5.1				102.1	0.020011
13_15	80.5 ± 4.6						31.0 ± 4.2					111.5	0.014419

Table S5. Wilcoxon test with a W statistic and Hodges Lehman estimator (difference in location) at a 95% confidence interval for total REE concentrations (ppm) between coal basins (PRB, ILB, or N. App), furnace type (opposed vs. tangential), or NOx technology (SCR vs no SCR). Results for Y-bulk composition based on bulk XANES (Y_2O_3, glass, hematite, or churchite) between furnace type or NOx technology.

Condition	p-value	W
Total REE concentrations		
SCR vs. no SCR	0.04	44
Tangential vs. Opposed	0.14	39.5
Y speciation determined by bulk XANES		
Y_2O_3: SCR vs. no SCR	0.67	6
Glass: SCR vs. no SCR	0.45	6
Hematite: SCR vs. no SCR	0.19	4
Churchite: SCR vs. no SCR	0.10	14
Y_2O_3: Tangential vs. Opposed	0.67	6
Glass: Tangential vs. Opposed	0.45	6
Hematite: Tangential vs. Opposed	1	8.5
Churchite: Tangential vs. Opposed	0.18	13

Table S6. Kruskal-Wallis test to determine if there is a statistical significance difference between all 3 coal basins (PRB, ILB, and N. App) and total REE concentration (ppm), rather than 2 at a time.

	p-value	χ^2
Total REE concentration (ppm)	0.36	2.05
Y speciation determined by bulk XANES (%)		
Y_2O_3	0.21	3.17
Glass	0.22	3
Hematite (Fe_2O_3)	0.32	2.39
Churchite ($YPO_4 \cdot H_2O$)	0.11	4.33

References:

(1) Garcia, E.; Liu, P.; Sanchez, J.; Lee, S.; Wang, Q.; Wen, Y.; Shivaprakash, S.; Burns, S.; Tang, Y. A survey study on arsenic speciation in coal fly ash and insights into the role of coal combustion conditions. *Applied Geochemistry* **2024**, *170*, 106095. DOI: https://doi.org/10.1016/j.apgeochem.2024.106095.
(2) Winburn, R.; Grier, D.; McCarthy, G.; Peterson, R. Rietveld Quantitative X-Ray Diffraction Analysis of NIST Fly Ash Standard Reference Materials. *Powder Diffraction* **2000**, *15*, 163-172. DOI: 10.1017/S0885715600011015.
(3) Liu, P.; Huang, R.; Tang, Y. Comprehensive Understandings of Rare Earth Element (REE) Speciation in Coal Fly Ashes and Implication for REE Extractability. *Environmental Science & Technology* **2019**, *53* (9), 5369-5377. DOI: 10.1021/acs.est.9b00005.
(4) Lucas, S.; Champion, E.; Bregiroux, D.; Bernache-Assollant, D.; Audubert, F. Rare earth phosphate powders RePO4·nH2O (Re=La, Ce or Y)—Part I. Synthesis and characterization. *Journal of Solid State Chemistry* **2004**, *177* (4), 1302-1311. DOI: https://doi.org/10.1016/j.jssc.2003.11.003.
(5) Elzinga, E. J.; Reeder, R. J.; Withers, S. H.; Peale, R. E.; Mason, R. A.; Beck, K. M.; Hess, W. P. EXAFS study of rare-earth element coordination in calcite. *Geochimica et Cosmochimica Acta* **2002**, *66* (16), 2875-2885. DOI: https://doi.org/10.1016/S0016-7037(02)00888-8.
(6) Cornell, R. M.; Schwertmann, U. *The iron oxides: structure, properties, reactions, occurrences and uses*; John Wiley & Sons, 2003.
(7) De Witte, B. M.; Uytterhoeven, J. B. Acid and Alkaline Sol-Gel Synthesis of Amorphous Aluminosilicates, Dry Gel Properties, and Their Use in Probing Sol Phase Reactions. *Journal of Colloid and Interface Science* **1996**, *181* (1), 200-207. DOI: https://doi.org/10.1006/jcis.1996.0371.